GEOPHYSICAL RESEARCH LETTERS, VOL. 27, NO. 15, PAGES 2289-2292, AUGUST 1, 2000

The subglacial cavity and implied dynamics under Nioghalvfjerdsfjorden Glacier, NE-Greenland

Christoph Mayer,[1] Niels Reeh,[2] Frederik Jung-Rothenhäusler,[1] Philippe Huybrechts [1] and Hans Oerter,[1]

Abstract. Seismic depth soundings on Nioghalvfjerdsfjorden Glacier (NFG), NE Greenland, reveal an overdeepened trough under the floating glacier. The maximum depth of the trough reaches more than 900 m below sea level. Mass balance calculations indicate considerable ice loss due to strong subglacial melting with a mean melt rate of $8\,\mathrm{m\,a^{-1}}$. The geometry of the cavity and water mass characteristics from CTD measurements suggest the existence of a well defined regional circulation system. Warm, saline and rather dense water follows the inward inclining basal slope through the deep valley of Dijmphna Sund towards the grounding line. Shallow ridges at the eastern glacier front prevent this water mass entering from that direction. The comparatively cold, fresh and less dense melt water follows the subglacial ice topography leaving the cavity through the gaps towards the east. The abundance of subglacial melt water east of NFG is most probably one of the main reasons for the semi permanent sea ice cover in this region. Cold water masses upwelling in the Northeast Water Polynia and detected by satellite remote sensing are very likely influenced and modified by the subglacial melt water production.

Introduction

The mass balance of the Greenland ice sheet is determined by accumulation and ablation on its surface and mass transport across the grounding line into floating ice tongues, where, for steady state conditions, melting and calving balance the mass input. In northern Greenland climatic conditions allow the formation of small ice shelves, whereas further south the calving front of outlet glaciers is close to their line of floatation. Ice shelves are observed for annual mean temperatures below -10° C and mean summer temperatures under 5° C [*Funder et al.*, 1998, Figs. 8-10]. For the floating part mass loss occurs also as subglacial melting, in addition to surface melting and calving at the ice front. Here, subglacial melting can be a substantial part of the overall mass loss [*Reeh et al.*, 1997]. General mass balance calculations need to include this subglacial melting in order to give realistic results.

Melting and freezing at the underside of floating ice masses depend on temperature, salinity and circulation of the water below [*Lewis and Perkin*, 1986]. Further, the circulation conditions are stronlgy influenced by the geometry of the subglacial cavity [*Grosfeld et al.*, 1997]. Antarctic Bottom Water, formed from subglacial melt water, influences e.g. the entire circulation system of the Atlantic Ocean [*Emery and Meinke*, 1986]. The production of a considerable amount of subglacial melt water from North Greenland ice tongues could influence at least the regional oceanographic conditions including the near shore sea ice extent.

To assess the effect of subglacial melting on ice dynamics and the regional oceanography, our multidisciplinary approach to the system included: the determination of ice flux and surface ablation, oceanographic measurements and the geophysical investigation of the sub-ice cavity. Fieldwork was accomplished in collaboration between the Geological Survey of Denmark and Greenland (GEUS), the Danish Center for Remote Sensing (DCRS), the Alfred Wegener Institute (AWI) and the Danish Polar Center (DPC). This paper will concentrate on the subglacial cavity, the conditions for water circulation and subglacial melt water production.

Measurements and Results

NFG, a major outlet glacier in Greenland, drains 8.4% of the ice sheet area [*Jung-Rothenhäusler*, 1998]. This glacier forms a floating ice tongue of roughly 60 km length and 20 km width, situated at 79.5° N and 19 - 22° W [*Thomsen et al.*, 1997, and Figure 1]. From the west the ice enters Nioghalvfjerdsfjorden from the ice sheet, descending from above 900 m to about 80 m a.s.l. within 40 km. To the east the glacier forms a 35 km wide calving front into the open sea, blocked at some locations by ice rumples or rock scarries. Part of the glacier branches off to the north and calves into the 10 km wide Dijmphna Sund. In addition, a minor part of the floating ice drains into Blåsø, a lake close to and north of the main grounding line. The general flow direction is approximately northeast and turns to east on the last 20 km. The floating part of the glacier shows strong surface melting during summer with annual mean ablation of more than $1\,\mathrm{m\,a^{-1}}$ of ice [*Thomsen et al.*, 1997].

The Results are derived from 98 seismic depth soundings and 15 CTD profiles, which have been measured during two field seasons (Figure 1). In addition, a detailed study of surface elevation and ice thickness was performed by DCRS using airborne laser altimetry and radio echo soundings (60 MHz).

Reflection seismics

In contrast to airborne radio echo sounding, surface bound seismic sounding is much slower, especially on difficult ground. Still, the seismic method is the only practical way to determine water depths underneath floating ice. Nevertheless, our chosen location pattern (Figure 1) for the single shots permits the generation of a rather complete subglacial basin geometry.

[1]Alfred Wegener Institute for Polar and Marine Research, Bremerhaven, Germany
[2]Danish Center for Remote Sensing, Technical University of Denmark, Lyngby, Denmark

Paper number 2000GL011514.
0094-8276/00/2000GL011514$05.00

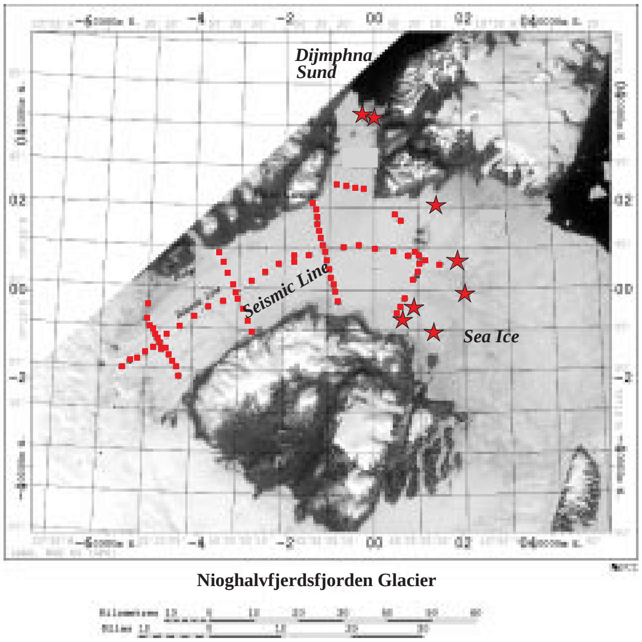

Figure 1. Geocoded Landsat Image of NFG. The dots represent seismic depth soundings, the stars CTD locations. Dijmphna Sund is ice free, whereas east of the glacier a semi-permanent sea ice cover exists.

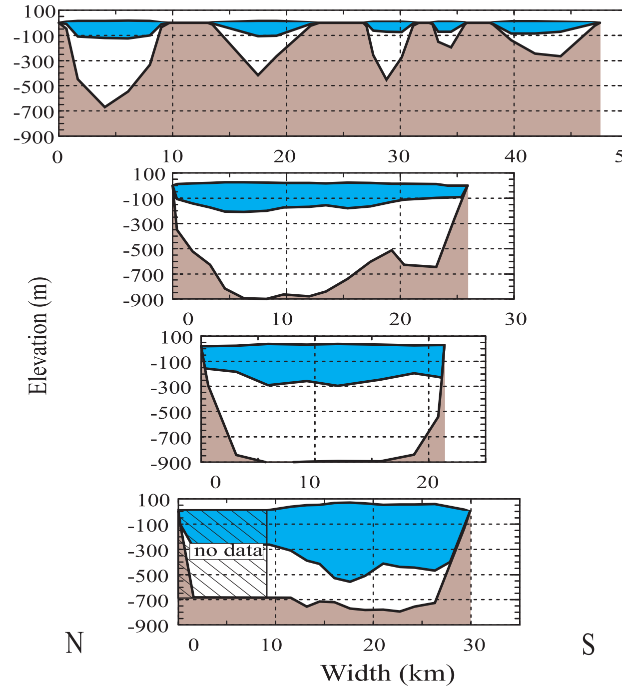

Figure 3. Ice thickness and sea bottom elevation from seismic soundings on fjord cross profiles at the ice front (top), close to Dijmphna Sund (upper middle), about half way of the glacier (lower middle) and close to the grounding line (bottom). Exact locations in Fig. 1.

The same setup was used for each seismic shot: 600 g explosives in 1 m deep boreholes acted as energy source at a distance of 100 m to the first of 24 geophones, evenly spaced at 10 m intervals. The reflection times were converted into distances by the following seismic p-wave velocites in ice and sea water: In the absence of a firn layer on the ice, the seismic p-wave velocity can be taken as 3800 m s^{-1} [*Robertson and Bentley*, 1990; *Kohnen*, 1974]. The mean sound velocity of the subglacial water was calculated from results of the CTD profiles to 1458 m s^{-1}.

The resulting ice thicknesses and bedrock elevations are shown in Figure 2 and Figure 3. Compared to the shallow shelf bathymetry in front of the glacier [*Perry et al.*, 1986], the sea bottom beneath the glacier forms a deep trough, starting at 600 m b.s.l close to the grounding line and deepening to more than 900 m half way between grounding line and glacier terminus. Close to the main glacier terminus, the sea bottom rises within 20 km from 800 m to 200 m b.s.l., in some parts even higher, forming several small ice rumples. In contrast, the water depth at the divergence into Dijmphna Sund is close to 600 m.

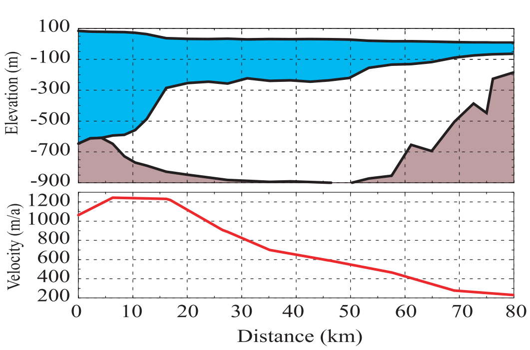

Figure 2. Ice thickness and sea bottom elevation along the longitudinal seismic profile (upper part) and the corresponding surface flow velocity from repeated GPS stake measurements (lower part). The drastic thinning close to the grounding line is not reflected in the flow velocity, which indicates strong changes in mass balance.

Along the seismic profile of Figure 2, which follows the main flow direction, the ice becomes afloat where its thickness reduces below 675 m. On this profile two remarkable thickness changes are observed. Close to the grounding line the ice thickness reduces by 330 m within 5 km. The second thinning starts at the opening of the fjord towards Dijmphna Sund. Here, the ice is not channeled anymore and is able to spread also transverse to the main flow. Simple ice dynamic calculations show that this is the main reason for the thinning from 258 m to 174 m over only a few kilometers. The cross profiles (Figure 3) show rather uniform ice thicknesses across the fjord. The spacing, equal to several ice thicknesses, between individual soundings possibly obscures high frequent thickness changes resolved by radio echo soundings close to the main grounding line.

CTD measurements

At the main glacier terminus, as well as in the Dijmphna Sund several CTD profiles have been measured (locations in Figure 1). A clear layering of water masses can be detected in all profiles (Figure 4). There was almost no sea ice covering Dijmphna Sund, which resulted in a warming of the uppermost 20–30 m due to high summer air temperatures (0–4° C) and solar radiation. Below this layer, cold water with salinities of about 32.6 is found, which could either be a mixture of sea water and subglacial melt water, or Polar

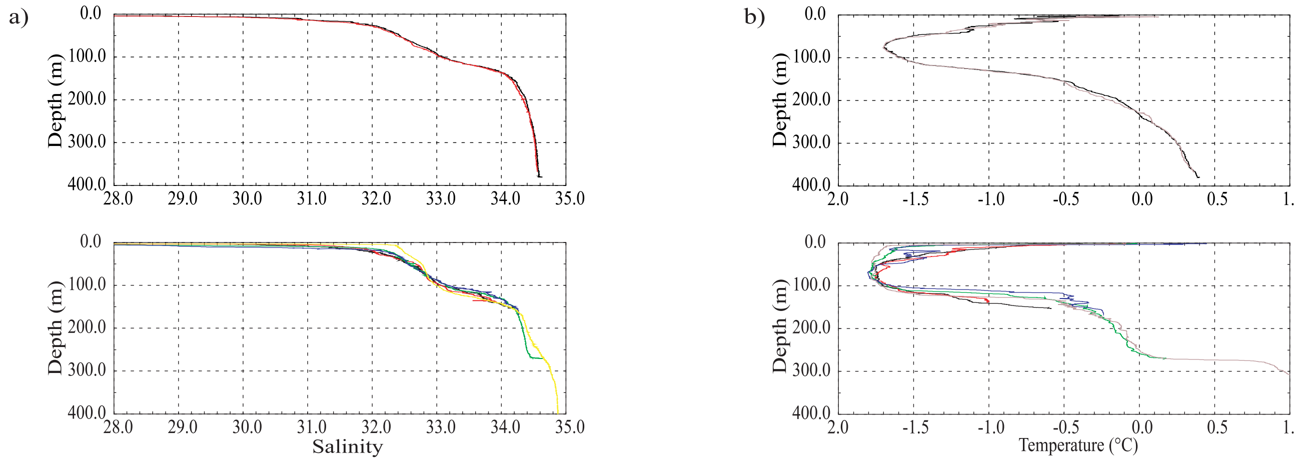

Figure 4. **a)** Salinity/pressure profiles and **b)** temperature/pressure profiles for the CTD mesaurements, both for Dijmphna Sund (top) and the main glacier front (bottom). Note: Salinities are given without units according to the Practical Salinity Scale 1978 [*UNESCO*, 1986].

Halocline Water, which is transported by the East Greenland current and formed in the presence of a polar ice cover [*Bignami and Hopkins*, 1997]. The layer from 150 m down to 380 m consists of warm and saline water [*Hopkins*, 1991, return Atlantic Intermediate Water], which has the potential to generate subglacial melting. The conditions at the main glacier terminus are rather similar, with somewhat colder temperatures and a larger gradient between the different layers close to the ice front. Here, also some ice platelets, indication of basal melting, have been found at one location. In this area the sea bed elevation under the glacier is in the order of 300 m b.s.l., probably less in the shallowest parts, not necessarily matched by the seismic soundings. Thus, the warm water mass (AIW) detected in deeper regions east of the glacier cannot penetrate the subice cavity as easy as in Dijmphna Sund.

As shown in Figure 5, there are considerable differences in the Temperature/Salinity (T/S) diagram between the two areas. The local maximum in salinity (28–29) for the Dijmphna Sund profiles represents the warm surface layer, already mentioned. In contrast, the profiles in front of the main glacier terminus, where the sea ice cover was almost 100 %, show temperatures 0.4 to 1.4° C lower for the same salinity range. Also for salinities between 31.0 and 33.2, which correspond to a water depth between 10 and 110 m (Figure 4a), the temperatures in Dijmphna Sund are up to 1.0° C warmer than at the main front. For higher salinities up to 34.3 (water depth: 110–350 m) the differences are small, although, the water in Dijmphna Sund is generally colder.

Discussion

The main feature in the ice thickness distribution is the strong gradient close to the grounding line. The mean surface mass balance in this area is -1.2 m a^{-1} and the ice flow, at least in the central part of the glacier, is almost parallel [*Thomsen et al.*, 1997]. Estimated basal melt rates close to the grounding line, using the continuity equation, mean ice thicknesses and measured velocities along the flow line (Figure 2), give peak values up to 40 m a^{-1}, which seem too high. Anyhow, these estimations indicate extremley strong melting, which is supported by general mass balance calculations: The mean basal melt rate, which is the difference between inflow (15 $km^3\,a^{-1}$), calving flux (-1.5 $km^3\,a^{-1}$) and surface melting (-1.2 m a^{-1} $\times$ floating ice area, 1400 km^2), divided by the area of floating ice, is on the order of 8 m a^{-1} [*Thomsen et al.*, 1997]. Maximum melt rates are expected to occur at the deepest parts of the floating ice close to the grounding line. There, the highest temperature difference occurs between the inflowing water (AIW, +0.3 to +0.5° C) and the pressure melting point at the ice base (-600 m: $-0.52°$ C). Supporting this, our calculations also show significantly less basal melting downstream of the first major thinning step. The melting of the calculated volume of ice (11.8 km^3) requires an energy of 3.6×10^{12} kJ. For a temperature difference of $\approx$ 1.0° C, 826 km^3 of water are needed for melting. The cross profile area of the water column beneath the ice extending into Dijmphna Sund, determined from seismic soundings, is 4 km^2. Following the assumption that the entire warm water, necessary for melting, enters the subglacial cavity through this cross section, the resulting inflow velocity would be 0.66 cm s^{-1} to match the mean melt rate of 8 m a^{-1}.

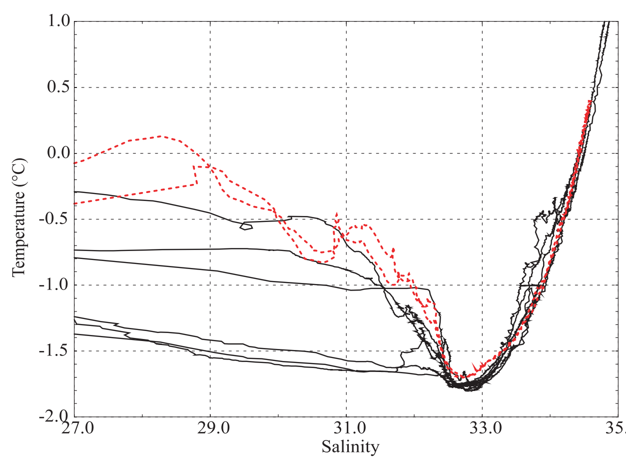

Figure 5. Temperature/salinity relation for CTD profiles in Dijmphna Sund (dotted) and at the main glacier front (bold). The most significant differences in water properties occur in the salinity range 27 to 32.

Because Dijmphna Sund is the widest and, more important, the deepest opening beneath the glacier it is very likely that most, if not all, warm and saline water required for the described high melt rates enters the cavity through this channel. Depth soundings in the northern part of Dijmphna Sund also exclude a shallow barrier which might prevent AIW transport from the open sea. The buoyant melt water moves along the largest gradient at the underside of the ice and thus along the main ice flow direction towards the eastern glacier terminus. This cold and less saline water (S: 31.8 to 32.5, T: -1.1 to -1.7° C in Figure 5), detected in the CTD profiles, will isolate and stabilize the semi permanent fast ice cover observed to the east of NFG [*Schneider and Budéus*, 1995] by stratifying between the sea ice and the warmer but denser water beneath.

In contrast to the direction of the East Greenland current a local northward current close to the coast exists in this area. The local occurence of cold and fresh water in the Northeast Water Polynia just north of the sea ice barrier was classified as East Greenland Shelf Water by Budéus et al. (1995). We suggest that this water mass is not only Polar Water modified by the inflow of regional surface melt water. It is strongly influenced by the subglacial melt water from NFG. A reduced inflow of AIW, or a cooling of this water mass would result in smaller subglacial melt rates and, surprisingly, in a reduced stablizing effect on the sea ice cover in front of the glacier.

Acknowledgments. We greatefully acknowlegde funding by the European Union (ENV4-CT095-0124). Many thanks also to the DPC and all colleagues for ideal working conditions, Gereon Budèus for his valuable comments on the oceanographic part and Astrid Lambrecht for perfect field communications. This is AWI contribution Nr. 1804.

References

Bignami, F. and T. S. Hopkins, The water mass characteristics of the Northeast Water Polynya: *Polar Sea* data 1992–1993, Journal of Marine Systems *10*, 139–156, 1997.

Budéus, G., W. Schneider and G. Kattner, Distribution and exchange of water masses in the Northeast Water Polynya (Greenland Sea), Journal of Marine Systems *10*, 123–138, 1997.

Emery, W. J. and J. Meincke, Global water masses: summary and review, Oceanologica Acta *9*(4), 383–391, 1986.

Funder, S., C, Hjort, J. Y. Landvik, S. Nam, N. Reeh, and R. Stein, History of a Stable Ice Margin - East Greenland during the Middle and Upper Pleistocene, Quaternary Science Reviews *17*, 77–123, 1998.

Grosfeld, K., R. Gerdes and J. Determann, Thermohaline circulation and interaction beneath ice shelf cavities and the adjacent open ocean, *J. Geophys. Res., 102*(C7), 15,595–15,610, 1997.

Hopkins, T. S., The GIN Sea–A synthesis of its physical oceanography and literature review 1972 – 1985, Earth Sci. Rev. *30*, 175–318, 1991.

Jung-Rothenhäusler, F., *Fernerkundungs- und GIS-Studien in Nordostgrönland*, Berichte zur Polarforschung *280*, Alfred-Wegener-Institut für Polar- und Meeresforschung, Bremerhaven, 1998.

Kohnen, H., The temperature dependence of seismic waves in ice, Journal of Glaciology *13*(67), 144–147, 1974.

Lewis, E. L. and R. G. Perkin, Ice pumps and their rates, *J. Geophys. Res., 91*(C10), 11756–11762, 1986.

Perry, R. K., H. S. Fleming, J. R. Weber, Y. Kristoffersen, J. K. Hall, A. Grantz, G. L. Johnson, N. Z. Cherkis and B. Larsen, Bathymetry of the Arctic Ocean, Geol. Soc. Am., Map Chart Ser., *MC-56*, 1986.

Reeh, N., H. Thomsen, O. Olesen and W. Starzer, Mass balance of North Greenland, Science *278*, 205–206, 1997.

Robertson, J. D. and C. R. Bentley, Seismic studies on the grid western half of the Ross Ice Shelf: RIGGS I and RIGGS II, *in* Bentley, C. R. and D. E. Hayes (ed.), *The Ross Ice Shelf: Glaciology and Geophysics*, Vol. 42 of Antarctic Research Series, Washington, DC, pp. 55–86, 1990.

Schneider, W. and G. Budéus, On the generation of the Northeast Water Polynya, *J. Geophys. Res., 100*(C 3), 4269–4286, 1995.

Thomsen, H. H., N. Reeh, O. B. Olesen, C. E. Bøggild, W. Starzer, A. Weidick and A. K. Higgins, The Nioghalvfjerdsfjorden glacier project, North-East Greenland: a study of ice sheet response to climatic change, Geology of Greenland Survey Bulletin *176*, 95–103, 1997.

UNESCO, Progress on oceanographic tables and standards 1983–1986, Tech. Pap. Mar. Sci. *50*, 59 pp, 1986.

C. Mayer, Now at: Institute for Meteorology and Geophysics, University of Innsbruck, Innrain 52, A-6020 Innsbruck, Austria. (e-mail: Christoph.Mayer@uibk.ac.at)

F. Jung-Rothenhäusler, P. Huybrechts and H. Oerter, Alfred Wegener Institute for Polar and Marine Research, Columbusstr., D-27568 Bremerhaven, Germany.

N. Reeh, Danish Center for Remote Sensing, Technical University of Denmark, DK-2800 Lyngby, Denmark.

(Received February, 18, 2000; accepted March, 30, 2000)